

## Electronic supplementary information

### Phosphonate monoesters on thiacalix[4]arene framework as potential inhibitors of protein tyrosine phosphatase 1B

Viacheslav V. Trush,<sup>a</sup> Sergiy G. Kharchenko,<sup>b</sup> Vsevolod Yu. Tanchuk,<sup>a</sup> Vitaly I. Kalchenko,<sup>b</sup>  
Andriy I. Vovk<sup>\*a</sup>

<sup>a</sup>Department of Bioorganic Mechanisms, Institute of Bioorganic Chemistry and Petrochemistry of National Academy of Sciences of Ukraine, Kyiv, Ukraine

<sup>b</sup>Department of Phosphoranes Chemistry, Institute of Organic Chemistry of National Academy of Sciences of Ukraine, Kyiv, Ukraine

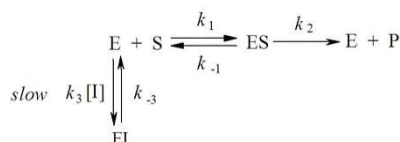
#### Table of contents

<b>Supplementary Methods</b>	S2
• Slow-binding inhibition	
• <i>In vitro</i> inhibition studies of PTPs	
• Molecular docking	
• Fluorescence measurements	
• Determination of quenching mechanism	
• Binding constant and binding site numbers	
• Thermodynamic parameters and binding forces	
• Synthesis of compounds	
<b>Supplementary Figures</b>	
Figure S1	S4
Figure S2	S4
Figure S3	S5
Figure S4	S6
Figure S5	S6
Figure S6	S7
<sup>1</sup> H, <sup>13</sup> C NMR and <sup>31</sup> P NMR spectra	S8
<b>References</b>	S11

### Slow-binding inhibition

Two mechanisms can be considered for explaining slow-binding enzyme inhibition.<sup>1</sup> In case of formation of EI complex in a single, slow step, the value of observed pseudo-first-order rate constant of association of inhibitor with enzyme ( $k_{app}$ ) increases linearly with increasing inhibitor concentration. Another mechanism assumes the rapid formation of EI complex and its slow isomerization to form more stable EI\* complex. This mechanism is characterized by hyperbolic relationship between  $k_{app}$  and inhibitor concentration.

Taking into account the behaviour of the slow-binding kinetics for compound **2** (Fig. S1), a one-step mechanism of enzyme-inhibitor complex formation can be assumed (Scheme).



Accordingly,  $k_{app}$  can be represented by the equation:<sup>1</sup>

$$k_{app} = k_{-3} + k_3 [I] / (1 + [S]/K_m),$$

where  $k_3$  and  $k_{-3}$  are association and dissociation rate constants for reversible enzyme-inhibitor complex formation, and

$$K_m = (k_{-1} + k_2) / k_1$$

### In vitro inhibition studies of PTPs

The enzymatic reactions were carried out at 37 °C (PTP1B) and 30 °C (TC-PTP, MEG1, MEG2 and SHP2). The assay solution contained 50 mM Bis-Tris (pH 7.2), 1 vol. % of dimethyl sulfoxide, 100 mM NaCl, 1 mM DTT, 3 mM EDTA, *p*-nitrophenyl phosphate, and the inhibitor. Concentrations of *p*-nitrophenyl phosphate were 2 mM (PTP1B, TC-PTP), 6 mM (Meg1, Meg2) and 7 mM (SHP2). The final volume was 0.5 ml. The mixture was preincubated for 5 min and the reaction was initiated by addition of the enzyme (6 nM in the reaction mixture). *p*-Nitrophenol released was determined by measuring the absorbance at 410 nm.

### Molecular docking

According to our previous study,<sup>2</sup> the conformations of PTP1B binding pocket can be divided into five clusters. Three of them are characterized by the conformations that have closed WPD-loop and another two are with open WPD-loop. Docking of the inhibitors has been done into all cluster centroids (1NL9 and 1PH0 with open WPD loop, and 2CNF, 1Q6M, and 2CM8 with closed WPD loop). After considering the predicted binding free energy values ( $\Delta G_{doc}$ ) and experimental activities of the inhibitors, the structure of PTP1B with closed WPD-loop (PDB entry 2CM8) was used to explain the enzyme-inhibitor interactions.

The enzyme-inhibitor interaction was studied using AutoDock 4.2 program.<sup>3</sup> Ligands and receptors were prepared using AutoDockTools. Initial 3D coordinates of the ligands were prepared using Chem Axon. The thiacalix[4]arene inhibitors are fixed in *flattened cone* conformation with angles between two opposite rings of approximately 150°, while other two aromatic rings are almost parallel to each other. In case of inhibitor **2** complexed to the enzyme, hydrogen bonds are observed between one of the phosphonate groups and Gly220 (2.7 Å), and Arg254 (3.1 Å). Another two phosphonate groups form hydrogen bonds with Lys116 (2.7 Å), Lys 120 (3.1 Å), Arg24 (2.8 Å) and Gln262 (3 Å).

### Fluorescence measurements

Fluorescence measurements were performed on a Varian Cary Eclipse fluorescence spectrophotometer. The fluorescence spectra were collected with a path length cell of 1 cm. The excitation and emission slits were set at 5 nm. The stock solution of HSA was prepared in 50 mM Tris-HCl buffer (pH 7.4). Intrinsic fluorescence was measured by exciting the protein solution at 280 nm.

### Determination of quenching mechanism

To identify the possible quenching mechanism, the experiments were carried out at 298, 308 and 318K, where HSA does not undergo any considerable thermal denaturation. The decrease in fluorescence intensity was analyzed using the Stern-Volmer equation:

$$F_0/F = 1 + K_{SV}[Q],$$

where  $F_0$  and  $F$  are the fluorescence intensities in the absence and presence of thiacalix[4]arene derivative, respectively.  $K_{SV}$  is the Stern-Volmer quenching constant and  $[Q]$  is the concentration of the added compound.

### Binding constant and binding site numbers

The binding constant ( $K_b$ ) and number of binding sites ( $n$ ) were calculated using the modified Stern-Volmer equation:

$$\log(F_0 - F/F) = \log K_b + n \log [Q],$$

where  $K_b$  and  $n$  are the binding constant and the average number of binding sites on HSA, respectively.

### Thermodynamic parameters and binding forces

The binding forces that play a major role in the ligand-protein complexation may include hydrogen bonds, electrostatic, van der Waals and hydrophobic interactions. According to the thermodynamic standpoint,  $\Delta H > 0$  and  $\Delta S > 0$  indicate hydrophobic interactions;  $\Delta H < 0$  and  $\Delta S < 0$  reflect the Van der Waals forces or hydrogen bond formation;  $\Delta H \approx 0$  and  $\Delta S > 0$  suggest electrostatic forces.<sup>4</sup> The thermodynamic parameters can be calculated from the van't Hoff equation:

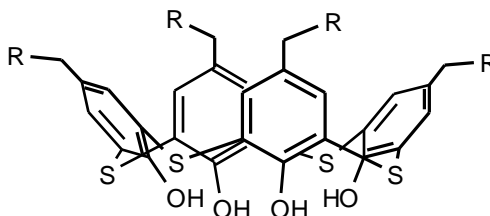
$$\ln K_b = -\Delta H/RT + \Delta S/R,$$

where  $K_b$  is the binding constant at the corresponding temperature (T), and R is the gas constant. The changes in enthalpy ( $\Delta H$ ) and entropy ( $\Delta S$ ) were determined from linear Van't Hoff plot (Fig. S6). The free energy change ( $\Delta G$ ) was estimated from the Gibbs equation:

$$\Delta G = \Delta H - T\Delta S$$

### Synthesis of compounds

Thiacalix[4]arene tetrakis(methylphosphonic) acid **1** was synthesized by treatment of tetrakis(diethoxyphosphorylmethyl)thiacalix[4]arene **4** with aqueous hydrochloric acid in accordance with the previously described protocol.<sup>5</sup> Tetraethyl and tetra-*n*-butyl monoester derivatives of thiacalix[4]arene tetrakis(methylphosphonic) acid (compounds **2** and **3**) were synthesized by previously reported method.<sup>6</sup> The reactions were carried out using octaethyl and octa-*n*-butyl esters of thiacalix[4]arene tetrakis(methylphosphonic) acid, respectively. Octaethyl ester of thiacalix[4]arene tetrakis(methylphosphonic) acid (compound **4**) and corresponding octa-*n*-butyl ester were synthesized by the Arbuzov reaction of chloromethyl thiacalix[4]arene with triethylphosphite or tri-*n*-butylphosphite (CHCl<sub>3</sub>, double excess of the phosphorylating agent), as described in detail in Ref.<sup>7</sup>



- 1** R<sup>1</sup>=PO(OH)<sub>2</sub>  
**2** R<sup>1</sup>=PO(OH)OEt  
**3** R<sup>1</sup>=PO(OH)O-*n*-Bu  
**4** R<sup>1</sup>=PO(OEt)<sub>2</sub>

<sup>1</sup>H, <sup>13</sup>C and <sup>31</sup>P NMR spectra were recorded on a Varian spectrometer operating at 400 MHz, 100 MHz and 121.5 MHz, respectively. The chemical shifts are reported using internal tetramethylsilane and external 85% H<sub>3</sub>PO<sub>4</sub> as references. Analytical thin layer chromatography was carried out on Silufol plates. The melting points were determined on a Boetius apparatus and are uncorrected.

### Synthesis of tetraethyl ester of thiacalix[4]arene tetrakis(methylphosphonic) acid (compound 2)

Suspension of octaethyl ester of thiacalix[4]arene tetrakis(methylphosphonic) acid (compound **4**, 1.0 g, 1.0 mmol) and LiBr (3.82 g, 44 mmol) in acetonitrile (65 ml) was stirred at boiling for 48 h. The reaction mass was cooled to room temperature. The precipitate was filtered off, washed with cold acetonitrile (2 × 10 ml). The resulting product – tetralithium salt of tetraethyl ester of thiacalix[4]arene tetrakis(methylphosphonic) acid – was dried in vacuum (0.01 mm Hg) at 75 °C for 2 h to obtain a colorless crystalline powder. Then the tetralithium salt (0.47g, 0.5 mmol) in water (35 ml) and 5 % solution of HCl (50 ml) were stirred at room temperature for 4 h. The precipitate was filtered, washed with water (2 × 10 ml) and dried in vacuum (0.01 mm Hg) for 4 h at 100 °C. Compound **2** was obtained as a light brown solid, yield 0.44 g (100%). Mp >250°C. <sup>1</sup>H NMR (400 MHz, DMSO-*d*<sub>6</sub>): δ 1.18 (t, 12H, *J* = 6.8 Hz, O-CH<sub>2</sub>-CH<sub>3</sub>), 2.96 (d, 8H, *J* = 20.8 Hz, CH<sub>2</sub>-P), 3.91 - 3.94 (m, 8H, O-CH<sub>2</sub>-CH<sub>3</sub>), 7.50 (s, 8H, ArH); <sup>31</sup>P NMR (121.5 MHz, DMSO-*d*<sub>6</sub>): δ 17.38. <sup>13</sup>C NMR (100 MHz, DMSO-*d*<sub>6</sub>): δ 16.40 (s, O-CH<sub>2</sub>-CH<sub>3</sub>), 31.77 (d, *J* = 126 Hz, P-CH<sub>2</sub>), 60.59 (s, O-CH<sub>2</sub>-CH<sub>3</sub>), 120.15 (s, Ar), 125.05 (s, Ar), 137.32 (s, Ar), 156.01 (s, Ar). Found, %: C, 44.25; H, 4.76; P, 12.28; S, 12.70. Calc. for C<sub>36</sub>H<sub>44</sub>O<sub>16</sub>P<sub>4</sub>S<sub>4</sub>: C, 43.90; H, 4.50; P, 12.58; S, 13.02.

### Synthesis of tetra-*n*-butyl ester of thiacalix[4]arene tetrakis(methylphosphonic) acid (compound 3)

Compound **3** was synthesized as described above. Octa-*n*-butyl ester of thiacalix[4]arene tetrakis(methylphosphonic) acid was transformed into tetralithium salt by interaction with LiBr in acetonitrile. At the second step, the tetralithium salt was hydrolyzed by HCl to compound **3**. Yield 0.53 g (100%). Mp >250°C. <sup>1</sup>H NMR (400 MHz, DMSO-*d*<sub>6</sub>): δ 0.86 (t, 12H, O-CH<sub>2</sub>-CH<sub>2</sub>-CH<sub>2</sub>-CH<sub>3</sub>), 1.26 - 1.37 (m, 8H, O-CH<sub>2</sub>-CH<sub>2</sub>-CH<sub>2</sub>-CH<sub>3</sub>), 1.45 - 1.60 (m, 8H, O-CH<sub>2</sub>-CH<sub>2</sub>-CH<sub>2</sub>-CH<sub>3</sub>), 2.97 (d, 8H, *J* = 22 Hz, CH<sub>2</sub>-P), 3.82 - 3.95 (m, 8H, O-CH<sub>2</sub>-CH<sub>2</sub>-CH<sub>2</sub>-CH<sub>3</sub>), 7.50 (s, 8H, ArH); <sup>31</sup>P NMR (121.5 MHz, DMSO-*d*<sub>6</sub>): δ 18.54. <sup>13</sup>C NMR (100 MHz, DMSO-*d*<sub>6</sub>): δ 13.53 (s, O-CH<sub>2</sub>-CH<sub>2</sub>-CH<sub>2</sub>-CH<sub>3</sub>), 18.36 (s, O-CH<sub>2</sub>-CH<sub>2</sub>-CH<sub>2</sub>-CH<sub>3</sub>), 32.10 (s, O-CH<sub>2</sub>-CH<sub>2</sub>-CH<sub>2</sub>-CH<sub>3</sub>), 31.73 (d, *J* = 127 MHz, P-CH<sub>2</sub>), 64.14 (s, O-CH<sub>2</sub>-CH<sub>2</sub>-CH<sub>2</sub>-CH<sub>3</sub>), 120.13 (s, Ar), 125.07 (s, Ar), 137.30 (s, Ar), 155.95 (s, Ar). Found, %: C, 48.62; H, 5.77; P, 11.54; S, 11.97. Calc. for C<sub>44</sub>H<sub>60</sub>O<sub>16</sub>P<sub>4</sub>S<sub>4</sub>: C, 48.17, H, 5.51; P, 11.29; S, 11.69.

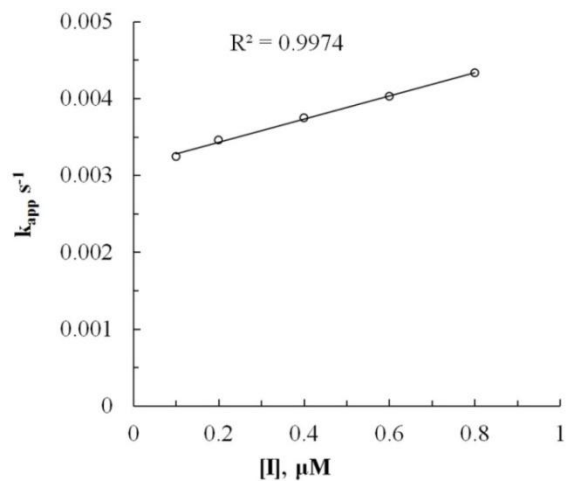


**Fig. S1** Dependence of apparent pseudo-first-order rate constant of the inhibitor association with PTP1B ( $k_{app}$ ) on inhibitor concentration (compound **2**).

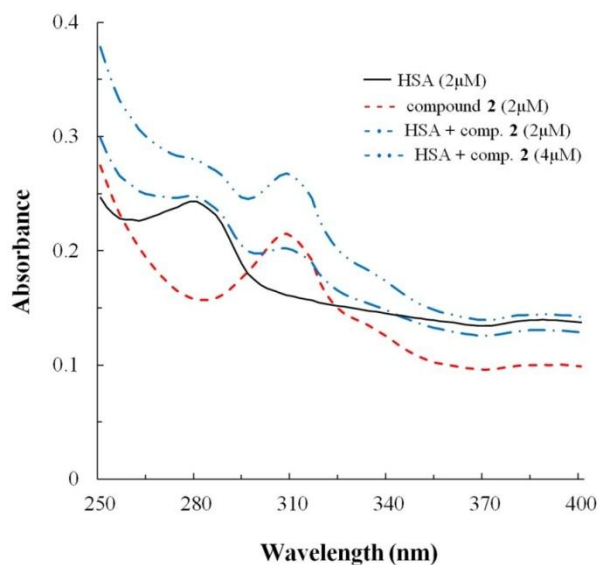


**Fig. S2a** UV-Vis spectra of HSA and HSA in the presence of compound **2**.

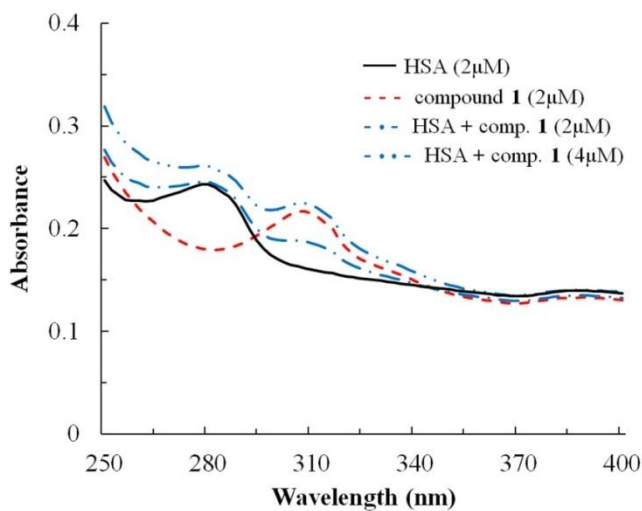


**Fig. S2b** UV-vis spectra of HSA and HSA in the presence of compound **1**.

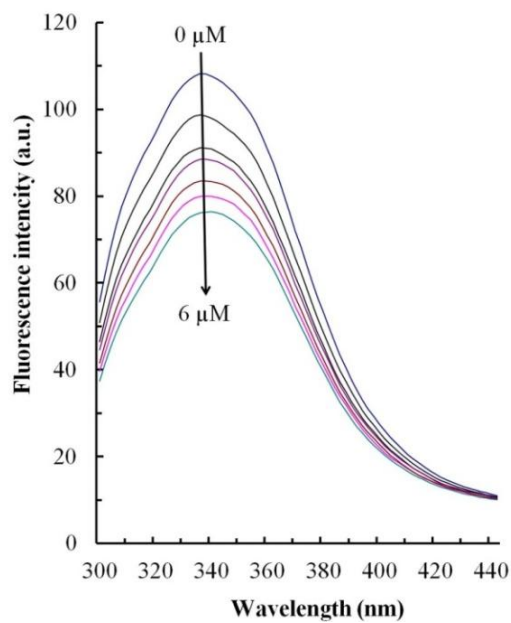


**Fig. S3a** Fluorescence spectra of HSA in the absence and in the presence of compound **1** at 298K. [HSA] = 2 μM, [**1**] = 0, 1, 2, 3, 4, 5, 6 μM.

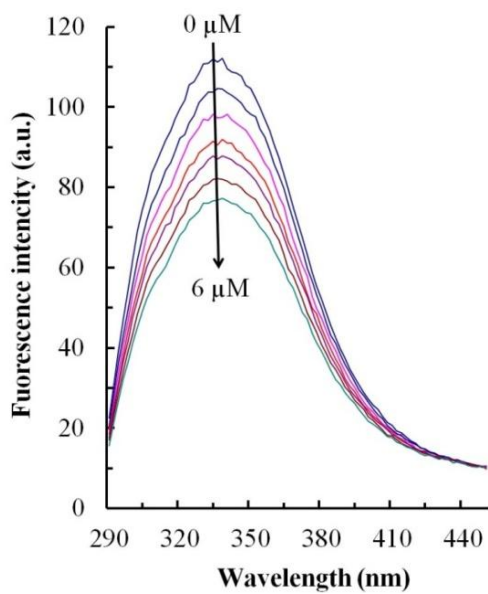


**Fig. S3b** Fluorescence spectra of HSA in the absence and the presence of compound **2** at 298K. [HSA] = 2 μM, [**2**] = 0, 1, 2, 3, 4, 5, 6 μM.

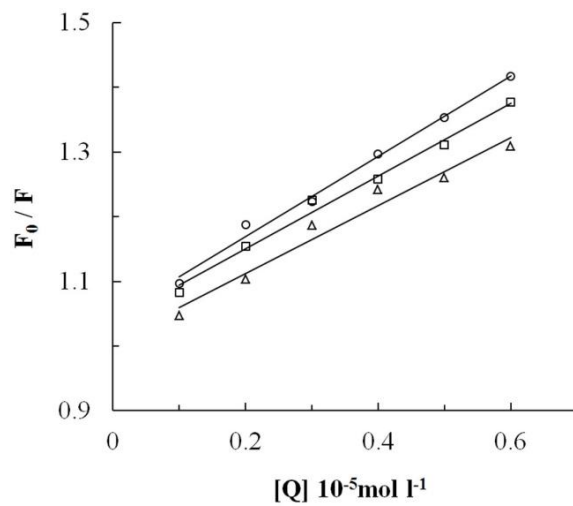


**Fig. S4a** Stern–Volmer plots for the quenching of HSA by compound **1** at 298K ( $\circ$ ), 308K ( $\square$ ), 318K ( $\Delta$ ), pH 7.4.

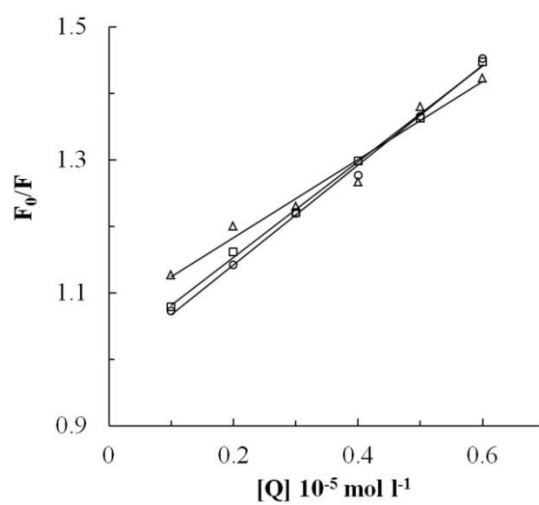


**Fig. S4b** Stern–Volmer plots for the quenching of HSA by compound **2** at 298K ( $\circ$ ), 308K ( $\square$ ), 318K ( $\Delta$ ), pH 7.4.

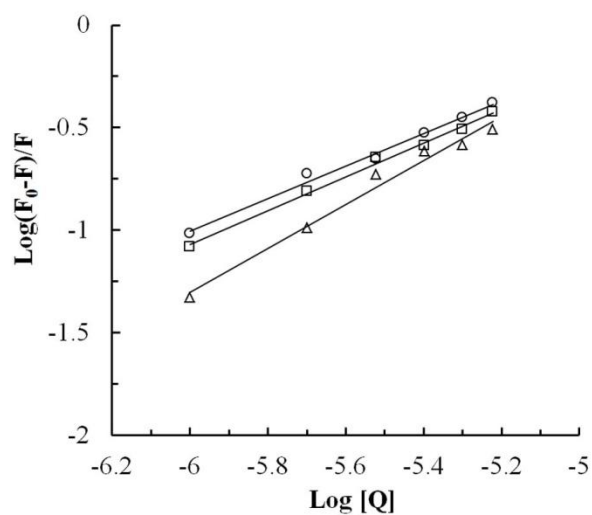


**Fig. S5a** Plots of  $\log(F_0-F)/F$  versus  $\log[Q]$  at 298K ( $\circ$ ), 308K ( $\square$ ), 318K ( $\Delta$ ) for compound **1**.

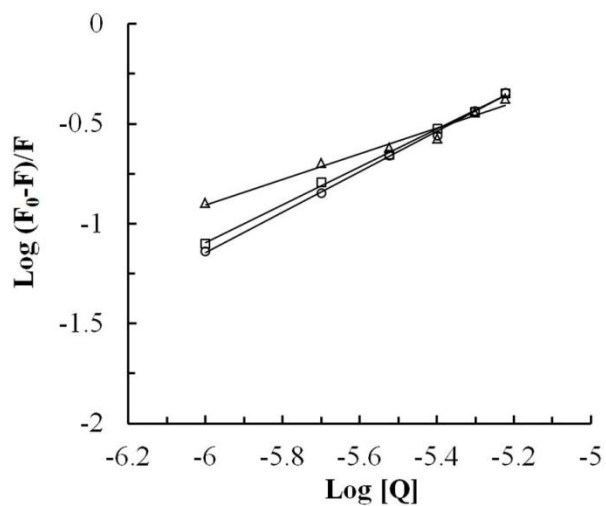


**Fig. S5b** Plots of  $\log (F_0-F)/F$  versus  $\log [Q]$  at 298K (○), 308K (□), 318K (Δ) for compound **2**.

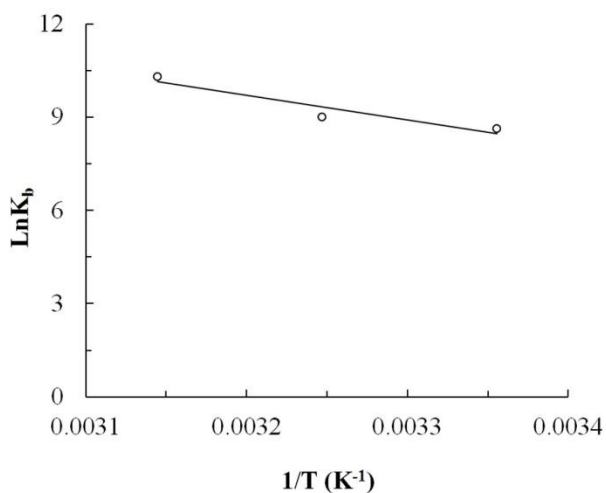


**Fig. S6a** Van't Hoff plot for the interaction of HSA with compound **1** in Tris-HCl buffer, pH 7.4.

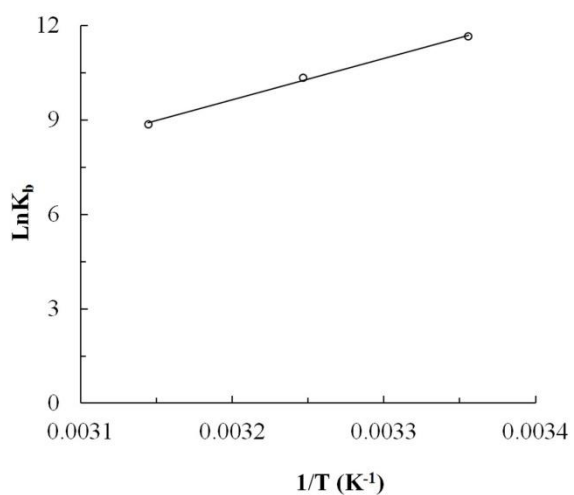
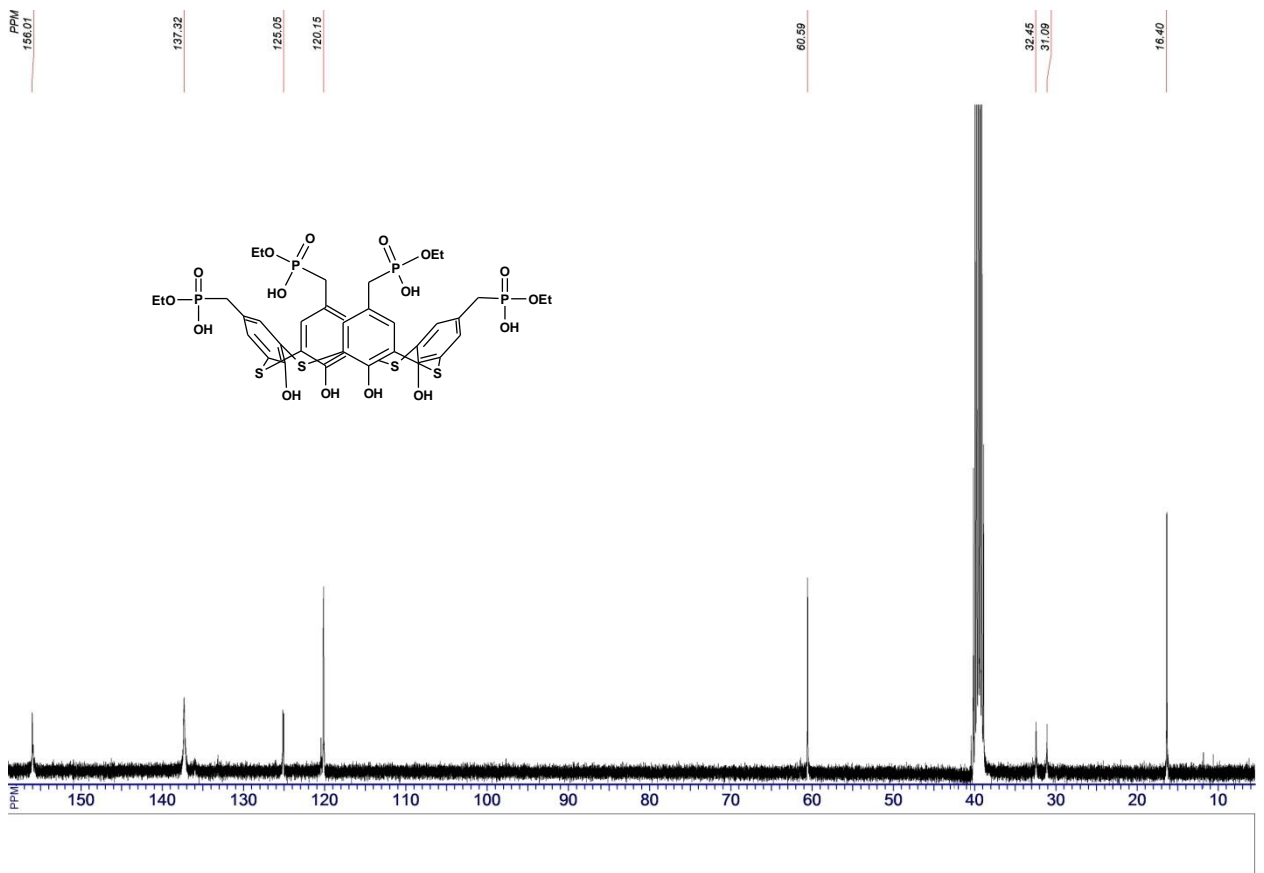
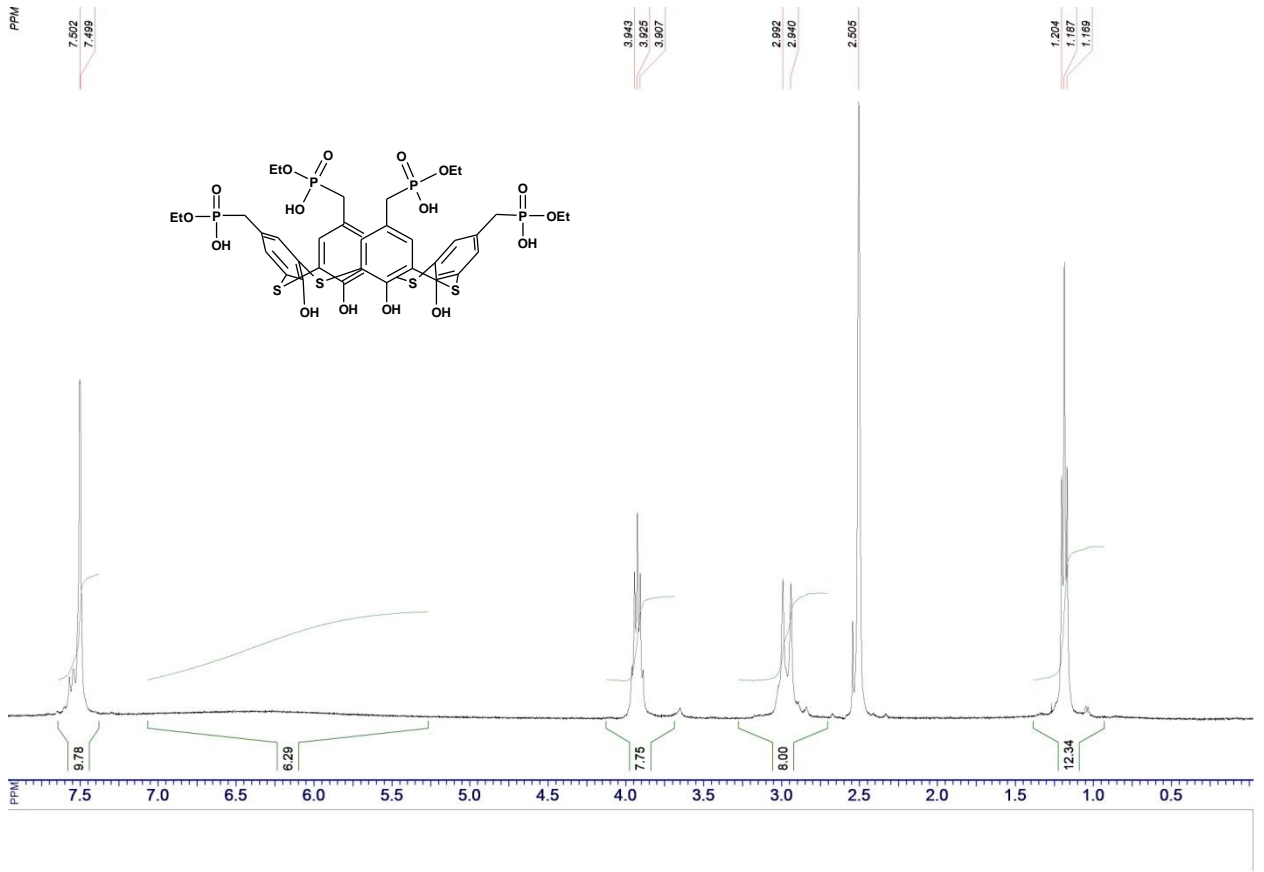
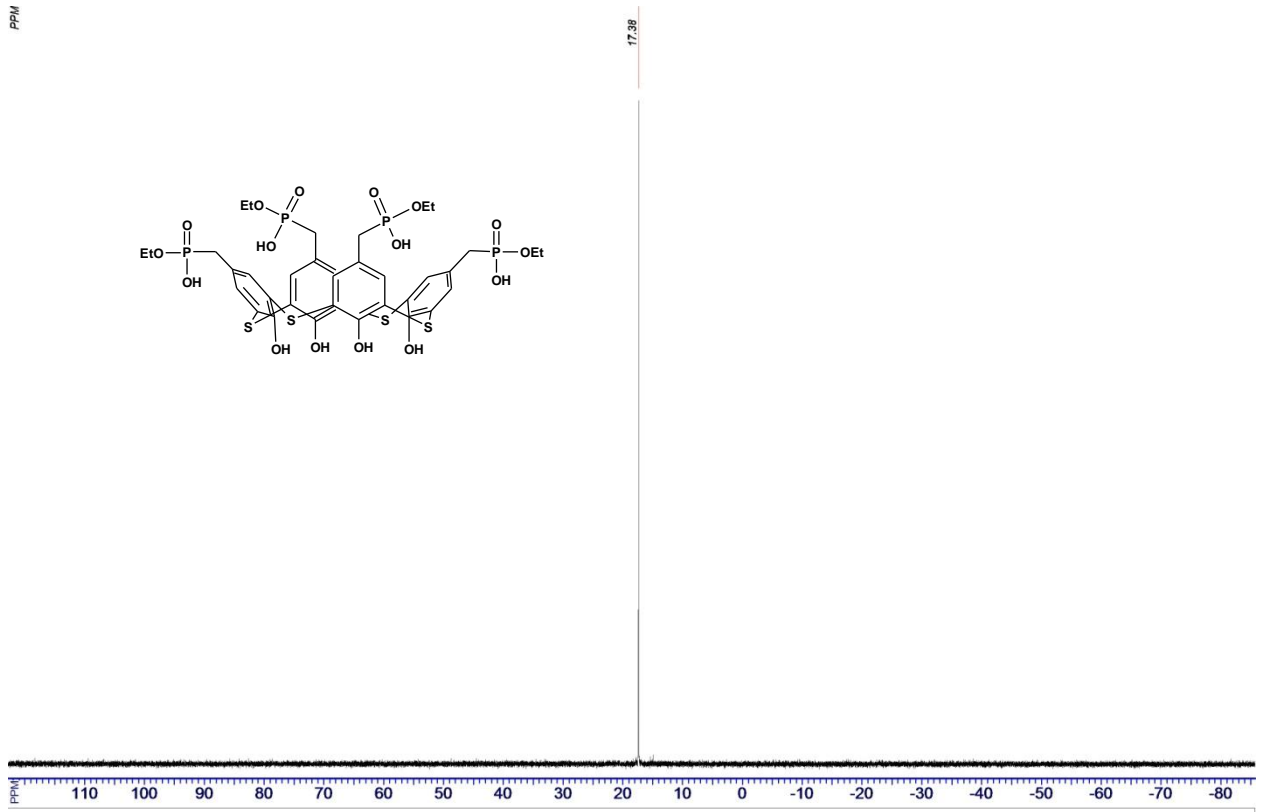
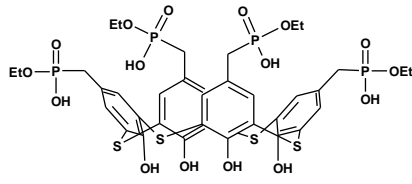


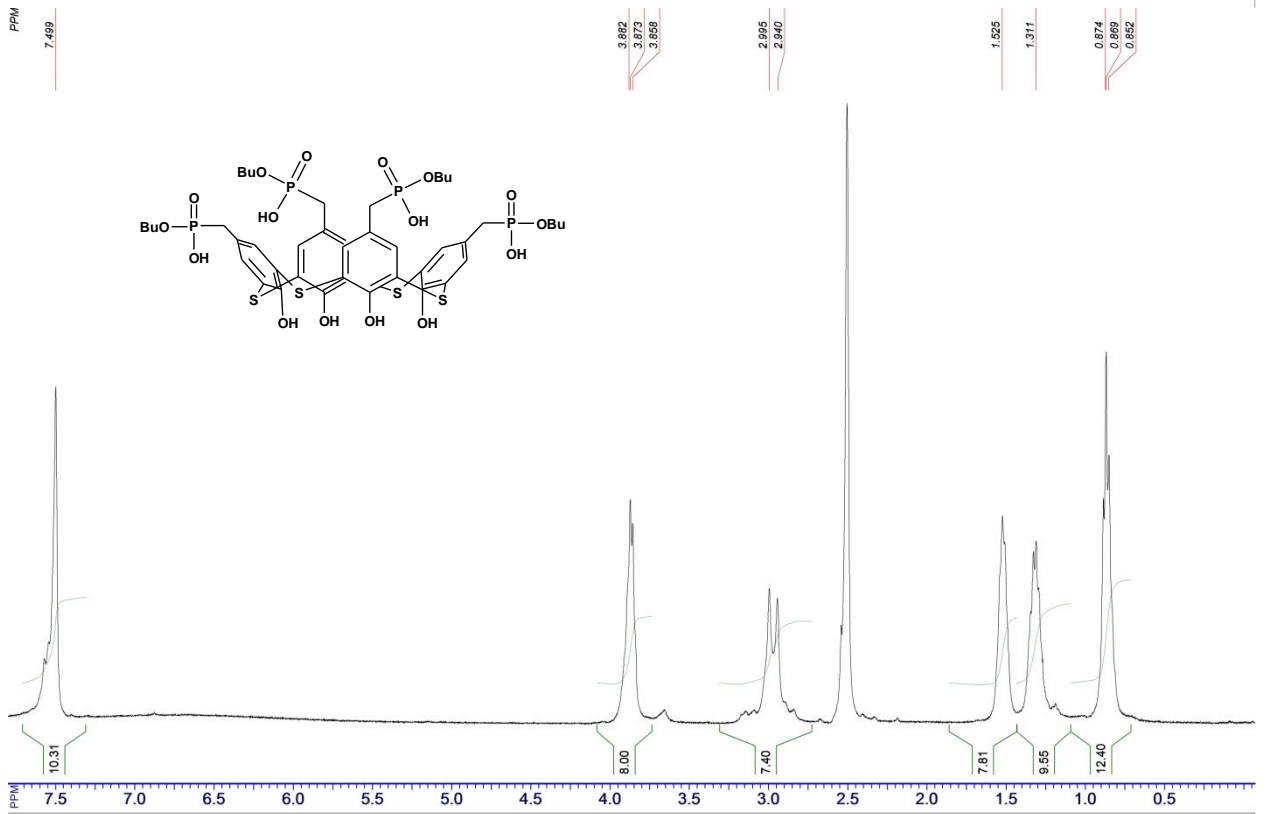
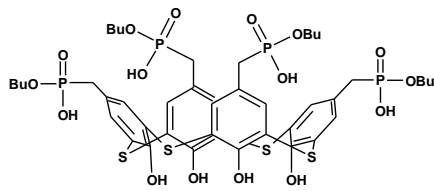
**Fig. S6b** Van't Hoff plot for the interaction of HSA with compound **2** in Tris-HCl buffer, pH 7.4.

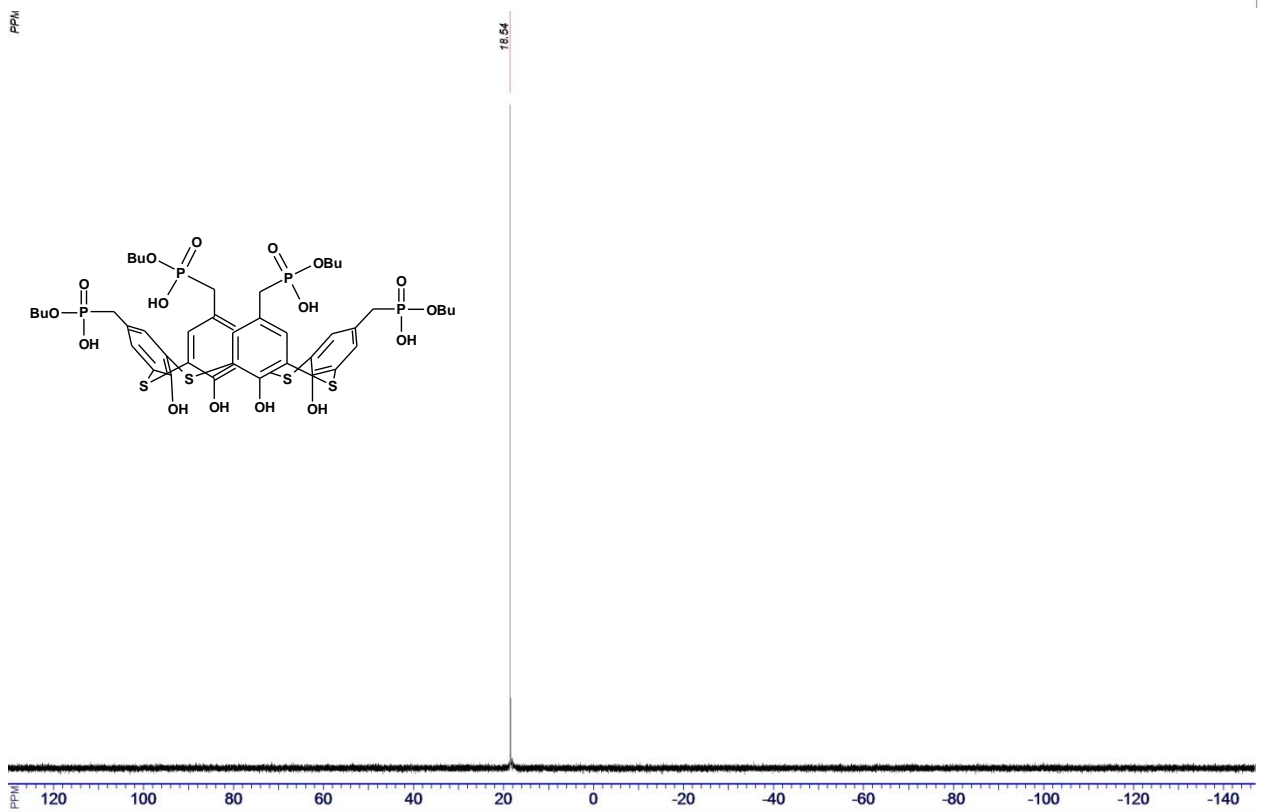
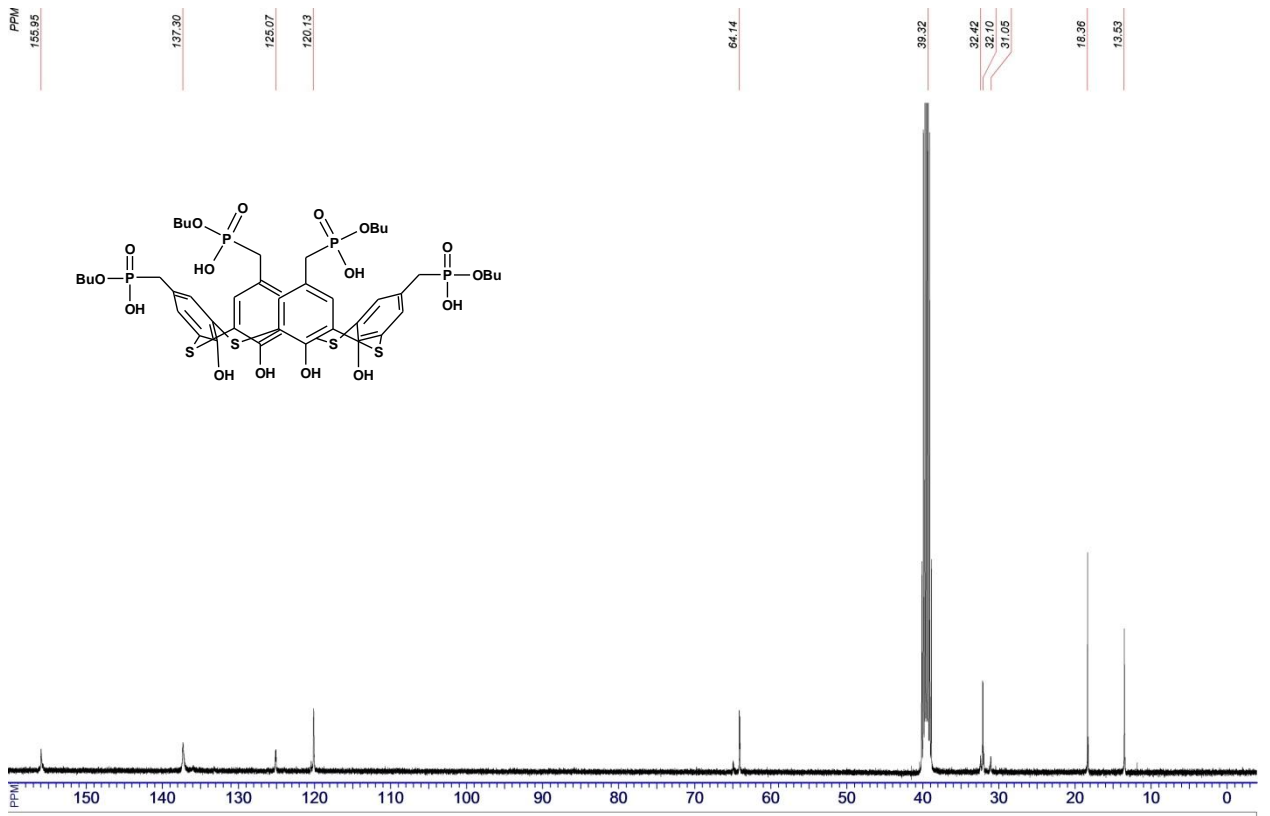


PPM



PPM





## References

---

- <sup>1</sup> M. Golicnik, J. Stojan, *Biochem. Mol. Biol. Educ.*, 2004, **32**, 228.
- <sup>2</sup> V. Y. Tanchuk, V. O. Tanin, A. I. Vovk, *Chem. Biol. Drug Des.*, 2012, **80**, 121.
- <sup>3</sup> R. Huey, G. M. Morris, A. J. Olson, D. S. Goodsell, *J. Comput. Chem.*, 2007, **28**, 1145.
- <sup>4</sup> P. D. Ross, S. Subramanian, *Biochem.*, 1981, **20**, 3096.
- <sup>5</sup> A. I. Vovk, L. A. Kononets, V. Y. Tanchuk, A. B. Drapailo, V. I. Kalchenko, V. P. Kukhar, *J. Inclusion Phenom. Macrocycl. Chem.*, 2010, **66**, 271–277.
- <sup>6</sup> S. G. Kharchenko, A. B. Drapailo, O. I. Kalchenko, G. D. Yampolska, S. V. Shishkina, O. V. Shishkin, V. I. Kalchenko, *Phosph. Sulfur Silicon*, 2013, **188**, 243-248.
- <sup>7</sup> O. Kasyan, D. Swierczynski, A. Drapailo, K. Suwinska, J. Lipkowski, V. Kalchenko, *Tetrah. Lett.*, 2003, **44**, 7167-7170.